Renewable Energy 42 (2012) 173–179

Contents lists available at SciVerse ScienceDirect

Renewable Energy

journal homepage: www.elsevier.com/locate/renene

Numerical and experimental studies on hydrofoils for marine current turbines

Jai N. Goundar [a], M. Rafiuddin Ahmed [a,*], Young-Ho Lee [b]

[a] Division of Mechanical Engineering, The University of the South Pacific, Suva, Fiji
[b] Division of Mechanical and Information Engineering, Korea Maritime University, Busan, South Korea

ARTICLE INFO

Article history:
Received 10 December 2010
Accepted 26 July 2011
Available online 3 September 2011

Keywords:
Marine current turbine
Cavitation number
Hydrodynamic characteristics
Lift
Drag
Pressure coefficient

ABSTRACT

The difficulty experienced by researchers while designing marine current turbine rotors is designing a superior-performance and cavitation free hydrofoil. The design of a high performance and cavitation free hydrofoil HF-Sx is presented in the present paper. Both numerical and experimental studies are carried out on the section. This hydrofoil can be used as the section of the outboard region of a horizontal axis 10 m rotor operating at a tip speed ratio of 4.3, determined using Blade element momentum theory. The section characteristics of HF-Sx as a blade section for 10 m are presented and its characteristics are compared with other hydrofoils used in marine current turbines.

1. Introduction

A horizontal axis marine current turbine (HAMCT) utilizes the kinetic energy of marine currents and converts it to mechanical energy. Energy from marine currents offers a regular and predictable source of renewable energy [1]. Using HAMCT to extract energy has less construction cost and the environmental impact compared to construction of tidal barrages. Tidal current technology is similar to wind energy technology [2]. However, there are several differences in the operating conditions. Under similar conditions, water is 830 times denser than air and water flow speed is much smaller [3]. There are also a number of fundamental differences in the design and operation of the marine turbine, which require further investigation, research and development. Particular differences are changes in Reynolds number, different stall characteristics and the possible occurrence of cavitation. However, useful information is available on the cavitation and stall characteristics of marine propellers [4]. This is very useful information for the design and analysis of marine turbines. Once the cavitation inception is avoided, then the blade element momentum theory (BEM theory) is assumed to be valid for an HAMCT [5]. BEM theory is widely used for predicting the performance of marine current turbines and the spanwise distribution of blade loading [6]. The BEM theory is well established for modeling rotor dynamics including marine propellers and wind turbines. BEM theory can be used to predict successfully spanwise loading on narrow blades, for wind and marine current turbines, but does not provide information on clockwise loading. Therefore other methods, such as 2D panel methods, can be used to study the stall characteristics and the occurrence of cavitation [6].

This paper describes the design of a new hydrofoil for HAMCT. This hydrofoil is designed to perform well at tip speed ratios (TSR) between 3 and 4 without having cavitation inception and also having good hydrodynamic performance of the turbine rotor. Experimental and numerical studies were done to obtain the hydrodynamic characteristics of HF-Sx. Having maximum thickness (t/c) of about 14.5%, the HF-Sx hydrofoil can be used as a blade section in the outer half of the blade. The hydrodynamic characteristics of HF-Sx were compared with other hydrofoils used for marine current turbines. The design method can be used to design hydrofoils for other Marine current turbines by studying these fundamental hydrodynamic characteristic of hydrofoils.

2. Hydrodynamic design parameters for hydrofoil

Hydrodynamic parameters for hydrofoil include studying the pressure distribution of the hydrofoil, minimum coefficient of pressure (C_P), coefficient of lift (C_L), coefficient of drag (C_D), and lift to drag ratio (L/D). Further design parameters include pitch, twist, and taper distribution of the blade and its performance characteristics on a rotating blade. The hydrodynamic design is further

* Corresponding author. Tel.: +679 3232042; fax: +679 3231538.
E-mail addresses: rafiuddin.ahmed@gmail.com, ahmed_r@usp.ac.fj (M.R. Ahmed).

0960-1481/$ – see front matter © 2011 Elsevier Ltd. All rights reserved.
doi:10.1016/j.renene.2011.07.048

Nomenclature

a	axial flow induction factor
a_0	tangential flow induction factor
A	rotor area (m^2)
c	chord (m)
C_D	drag coefficient ($D/½\ \rho AW^2$)
C_L	lift coefficient ($L/½\ \rho AW^2$)
C_P	coefficient of pressure ($P_L - P\infty$)/($0.5\ \rho AW^2$)
D	drag (N)
g	acceleration due to gravity (m/s^2)
h	is the local head of water at the blade tip immersion (m) $h = h_t + R - r$
h_t	is the tip immersion depth
L	lift (N)
P	rotor power (W)
P_L	local pressure (N/m^2)
$P\infty$	free stream static pressure (N/m^2)
P_V	vapor pressure of sea water (N/m^2)
P_{AT}	atmospheric pressure (N/m^2)
r	radius of local blade element (m)
R	blade radius (m)
t	thickness (m)
T	rotor trust (N)
V_u	uncorrected free stream velocity (m/s)
W	relative velocity of rotating blade $\sqrt{U_o^2(1-a)^2 + \Omega^2 r^2(1+a')^2}$
α	angle of attack of the water flow on the hydrofoil
ρ	density of sea water (Kg/m^3)
ε^{sb}	solid blockage correction factor
K_1	wind-tunnel correction constant for solid blockage effects (0.74)
M_v	model volume (m^3)
Ω	rotational speed (rad/s)
U_0	free stream velocity (m/s)
CPw	Power Coefficient $= P/(0.5\ \rho AW^2)$

complicated due to non-uniform speed and direction of the current, the shear profile in the tidal flow, and the influence of water depth and the free surface [7]. To study the section performance of the hydrofoil, the 2D panel code XFoil [8] was used. XFoil is a linear vorticity stream function panel method with viscous boundary layer and wake model, and is found to be suitable for predicting cavitation criteria at the preliminary design stage [9]. To make the HAMCT perform well over a wide range of conditions, a wide range of high C_L is needed, with delayed separation and stall. For better efficiency of the HAMCT, a lower C_D is required. For structural requirements, however, a thick section near the root is needed. For the case of marine current turbines it is important to have a section profile such that cavitation inception is delayed. Cavitation causes structural damage to turbine blades and reduces its performance; it causes lift to decrease and drag to increase, the pressure associated with bubble collapse is higher enough to cause failure of metals [10]. Cavitation inception is assumed to occur on the section when the minimum local pressure on the section falls below the vapor pressure of the fluid. Cavitation inception can be predicted by comparing the local minimum C_P with the cavitation number σ [4]. There will be cavitation on the hydrofoil if the local minimum C_P is lower than $-\sigma$. The cavitation number is defined as

$$\sigma = \frac{p_O - p_V}{0.5\ \rho W^2} = \frac{P_{AT} + \rho g h - p_V}{0.5\ \rho W^2} \quad (1)$$

The chances of cavitation occurring on the blade section increase more toward the tip of the turbine blade due to low immersion depth near the tip and the highest relative velocity experienced near the tip of the blade. This also results in higher Reynolds number (Re). Higher free stream velocity is experienced near the sea water surface compared to seabed; also the temperature of sea water is higher at the surface, which increases the chances of cavitation. Higher seawater temperature is experienced in hot countries like Fiji and other South Pacific countries throughout the year. These put challenges in designing hydrofoils to avoid cavitation, while maintaining higher L/D ratio and delayed stall characteristic for HAMCT. Delayed stall is important since higher turbulence and relative velocity at different angles can be experienced on rotating turbine.

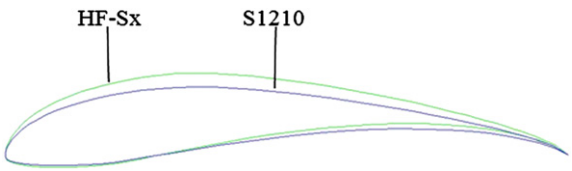

Fig. 1. Hydrofoil HF-Sx modified from S1210.

3. Hydrofoil design concept

Hydrofoils can be designed by studying the airfoil characteristics and modifying its shape to make it work at the required condition for marine current turbines. For designing the hydrofoil, 2-D panel method XFoil was used. Several airfoils were selected and their hydrodynamic characteristics such as C_P, C_L and C_D were studied. Airfoils selected were from the Eppler series, martin Heppele series, Selig series and Selig/Donovan series. A good hydrofoil for marine turbine applications must have a high lift to drag ratio for better performance and a higher C_P (lower suction) on the suction side to

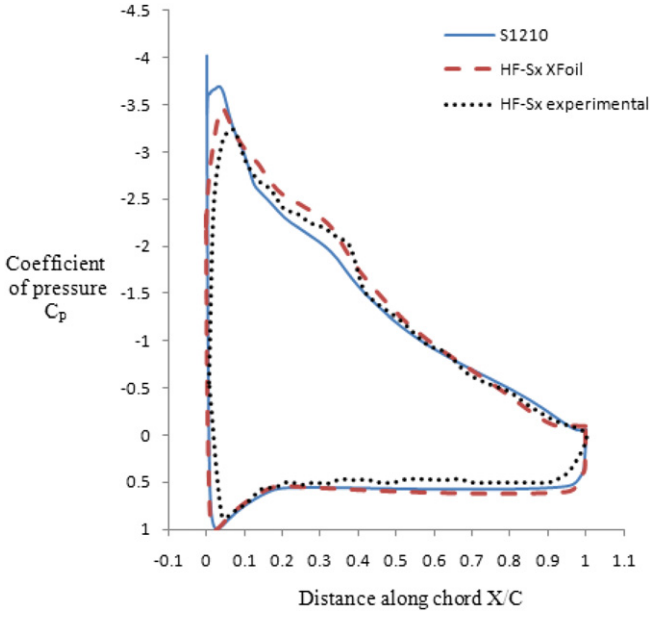

Fig. 2. Experimental and XFoil values of pressure distribution of HF-Sx and S1210 at 10° angle of attack and Re 190,000.

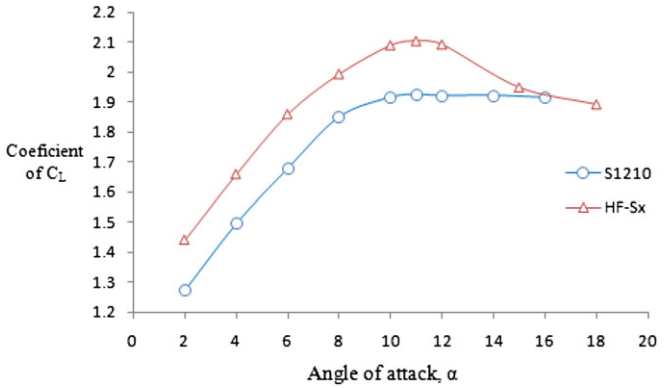

Fig. 3. Coefficient of lift at different angles of attack for HF-Sx and S1210 for Reynolds number of 190,000.

prevent cavitation. Selected airfoils from the above series were modified by changing their nose radius, maximum camber and maximum thickness to improve their hydrodynamic characteristics. From a number of modified airfoils, it was seen that the modified S1210 airfoil with increase in chamber by 20% and thickness by 20% was best optimized to work as a hydrofoil for marine current turbines. The optimized hydrofoil is named as HF-Sx and profile can be seen in Fig. 1. Increasing the camber and maximum thickness of airfoil increases its minimum C_P, can be seen in Fig. 2, minimum C_P of s1210 at 10° angle of attack (α) is about −4 and for HS-Sx it has increased to about −3.5. This will prevent the cavitation; however the lost area in increasing the suction pressure is gained as the C_p between minimum C_P and the Kink (transition point) increases, hence increased C_L and reduced C_D of the hydrofoil can be seen from Figs. 2 and 3. Hf-Sx has higher C_L and slightly lower C_D compared to S1210, it also has higher thickness compared to s1210 providing more strength to the blade structure (Fig. 4).

4. Experimental studies

The optimized hydrofoil Hf-Sx was fabricated in the laboratory with chord of 100 mm, span length of 300 mm for the 2-D laboratory scale testing. Pressure tubes were inserted on the surface to get the pressure distribution on the top and the bottom surfaces, and C_L and C_D of hydrofoil. The experiments were performed in an Engineering Laboratory Design (ELD) Inc., low speed open circuit wind tunnel. The Reynolds number of airflow in the wind-tunnel test section was matched with seawater flow velocity. Airflow at

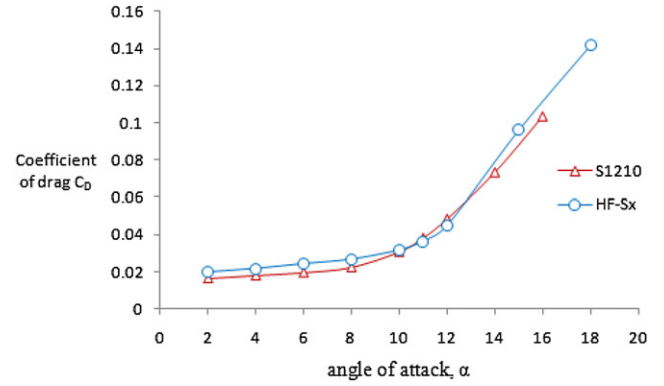

Fig 4. Coefficient of drag for HF-Sx and S1210 at different angles of attack and Reynolds number of 190,000.

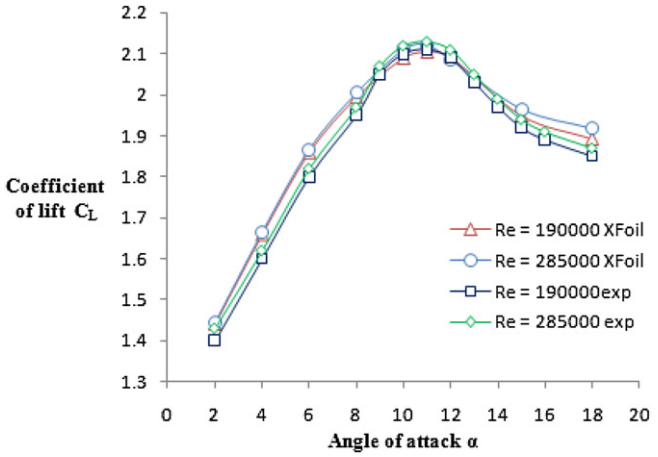

Fig. 5. Experimental and XFoil values of coefficients of lift.

speeds below 100 m/s is considered as incompressible flow, the maximum velocity of the wind tunnel is 49 m/s, and therefore all experiments were carried out at incompressible flow. Experiments on the hydrofoil HF-Sx were carriedout at two Reynolds numbers (Re), Re = 190,000 and 285,000, corresponding to seawater flowing at 2 m/s and 3 m/s. Solid blockage caused by the walls of the test section increases the flow velocity in the test section. The solid blockage was corrected using Equations (2) and (3) [11].

$$V = V_u\left(1 + \varepsilon^{sb}\right) \tag{2}$$

$$\varepsilon^{sb} = \frac{k_1(m_v)}{(csa)^{3/2}} \tag{3}$$

where csa is the cross-sectional area of the wind-tunnel test section.

Coefficient of pressure, lift and drag were determined experimentally and compared with XFoil results. Fig. 2 shows that there is good agreement between experimental and XFoil pressure distributions. Also there is good agreement between C_L and C_D obtained experimentally and with XFoil, as can be seen from Figs. 5 and 6. The XFoil results are verified with experimental results so XFoil can be used to determine the section characteristics of hydrofoils at higher Re. In actual conditions when the blade is rotating, the

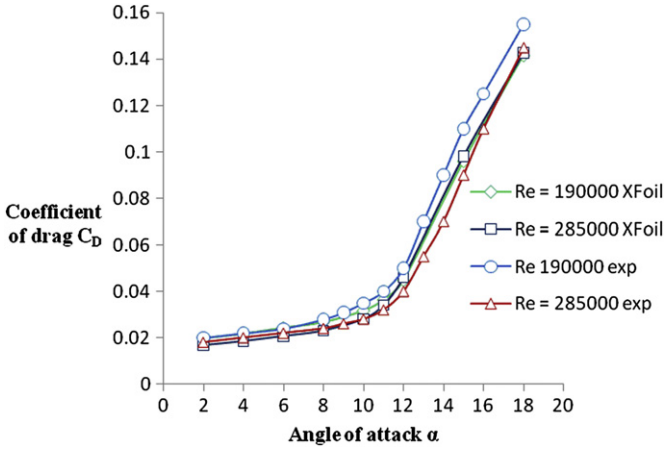

Fig. 6. Experimental and XFoil values of Coefficient of drag.

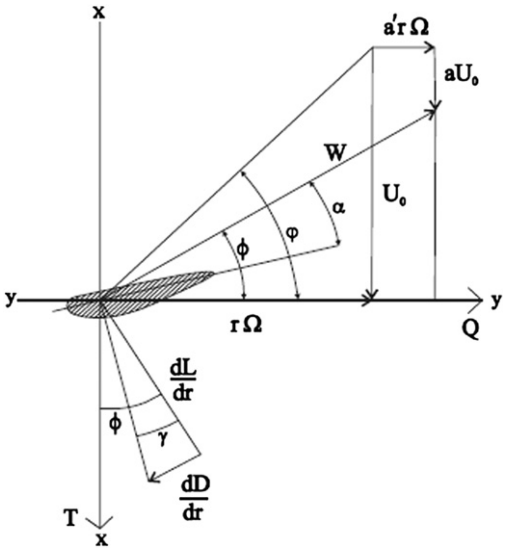

Fig. 7. Hydrodynamic component of forces and velocities on horizontal axis marine current turbine.

Reynolds number is significantly higher toward the tip, compared to freestream velocity near the blade root.

5. Hydrofoil characteristic for 10 m rotor

The characteristics of hydrofoils on rotating turbine behave differently. Once the rotor is in motion, the blade section starts to experience a relative component of tidal current velocity at variable angles of attack depending on blade parameters. Also, the hydrofoil section experiences different components of forces. The direction of tidal current velocity, blade forces and angle are shown in Fig. 7. These components of forces and velocities can be used to predict theoretical rotor performance, using the Blade Element Momentum (BEM) theory. The general BEM theory is based on a combination of momentum and blade element theories. The momentum theory is used to derive the axial and tangential inflow factors with inclusions of tip loss factors to take into account the finite number of rotor blades. The blade element theory is used to model the blade section drag and torque by dividing the rotor blade into a number of elements. The details and derivation of blade element momentum theory are given in Ref. [12]. The BEM theory does not account for cavitation inception on the blade section, therefore cavitation criteria needs to be predicted before applying BEM theory for HAMCT, and blades twist toward the tip needs to be modified to avoid cavitation inception. The hydrofoil angle at the tip may not be set to maximum lift, but at lower angle depending on the cavitation number at the tip to avoid cavitation. Some essential investigations and parametric studies have been done for design of 10 m rotor for HAMCT. Assumptions and approximations were done on rotor to perform with minimum control. The turbine is designed for a selected location known as Wilkes passage. The Wilkes passage is located west of the Fiji Islands close to Malolo Island, Fiji. Initial assessment was done at this location, a maximum tidal current of about 2 m/s at a depth of 2 m and a maximum depth of about 35 m were determined from the initial assessment. A 10 m rotor is chosen, as most of the tidal current energy is available at the upper half of the tidal streams [6]. A clearance of 5–7 m is taken for wave and low tide allowances. HF-Sx has been used as a hydrofoil section for 10 m rotor HAMCT. HF-Sx has maximum thickness (t/c) of about 14.5% therefore this section is appropriate for the outer half of the blade. For the root region, it is more appropriate to use thicker section of about 20–30% to have good strength to withstand the force acting on the blade by the moving water. HF-Sx can work best with lower TSR mostly between 3 and 5 without having cavitation inception and giving higher performance. The Power Coefficient (CP_w) of the rotor was calculated using BEM theory for 2 and 3 bladed rotors. This may not give the exact power compared to actual situation, but it is useful while designing the rotor, because it gives the performance approximation to chose the best design. By using 3 blade rotor maximum power can be extracted at lower TSR that can be seen in Fig. 8. As the TSR increases the chances of cavitation at the blade sections also increases, this is because the cavitation number decreases. It is better to keep the TSR of HAMCT lower to obtain higher performance without having cavitation. Three-bladed design and a TSR ratio of 4.3 were chosen; the

Table 1
Rotor parameters.

r/R	C (distri)	σ	Twist distri	C_L	C_p min
0.5	0.4375	14.75	13.04	2.145	−3.4713
0.55	0.41875	12.39	11.44	2.1483	−3.4821
0.6	0.4	10.51	10.01	2.1504	−3.4909
0.65	0.38125	8.99	8.73	2.1517	−3.5017
0.7	0.3625	7.75	7.58	2.1521	−3.5058
0.75	0.34375	6.74	6.54	2.1532	−3.5144
0.8	0.325	5.89	5.6	2.1544	−3.5232
0.85	0.30625	5.18	4.75	2.1558	−3.5321
0.9	0.2875	4.58	4.5	2.1502	−3.4231
0.95	0.26875	4.06	4.5	2.1219	−3.2814
1	0.25	3.63	4.5	2.0874	−3.1257

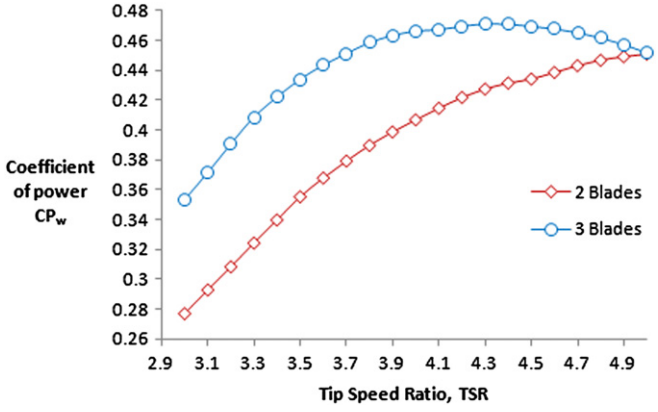

Fig. 8. Power coefficient of 2 and 3 Blade rotor using BEM theory.

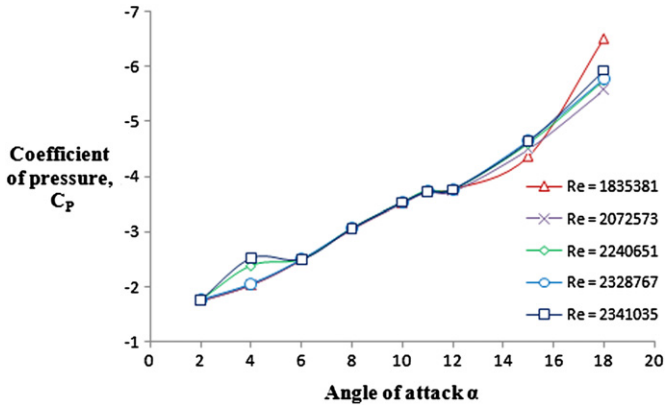

Fig. 9. Minimum coefficient of pressure for hydrofoil HF-Sx.

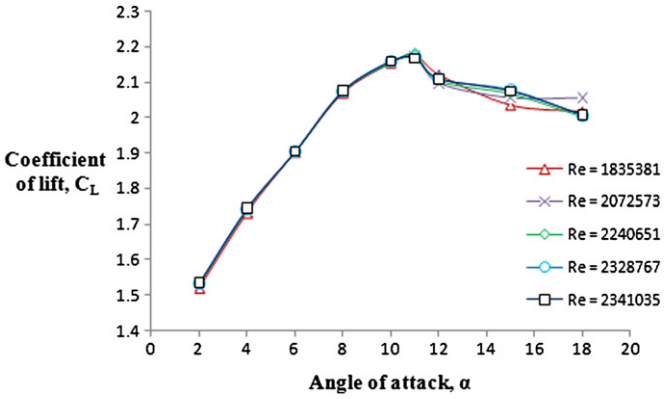

Fig. 10. Coefficient of lift for hydrofoil HF-Sx at different Reynolds numbers.

maximum power of the 3 bladed rotor is at TSR of 4.3, as can be seen from Fig. 8. Sea water properties were taken at 40 °C. It is assumed that this is the maximum sea water temperature for Fiji and the South Pacific. Other parameters such as chord distribution, twist distribution, cavitation number, coefficient of lift and pressure, used for rotor design are shown in Table 1. The hydrodynamic characteristics of rotors were determined using XFoil. Hydrofoil HF-Sx has a maximum lift at around 10°–11° AOA, from half of the blade to the tip, as can be seen from Fig. 10. Maximum C_L of the sections is slightly above 2.1. Minimum coefficient of pressure at different Reynolds numbers at maximum C_L is approximately −3.6, as can be seen in Fig. 9. It has a lower C_D at different angles of attack as can be seen from Fig. 11. HF-Sx can be effectively used in 10 m, three-bladed rotor, from $r/R = 0.5$ to the tip to maximize rotor performance and avoid cavitation. It can also be used for rotors having higher Reynolds numbers at the tip; however the twist at the tip needs to be modified to have − C_P minimum above the cavitation number near the rotor tip. Since HF-Sx is having significantly higher C_L and L/D at lower angle of attacks the rotor will have good performance even with the modified twist near the rotor tip.

5.1. Characteristics HF-Sx compared with other hydrofoils

The hydrodynamic characteristics of different hydrofoils were studied at a Reynolds number of 2,100,000 (which is the *Re* toward the tip of the HAMCT with 10 m diameter). The minimum coefficient of pressure of different hydrofoil at different angle of attack can be seen from Fig. 12. The C_L and C_D variations of different

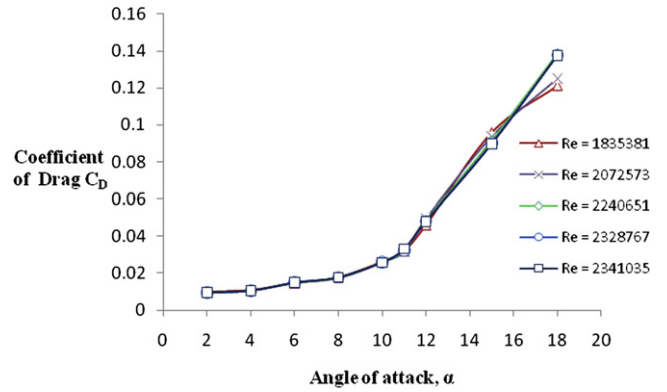

Fig. 11. Coefficient of drag for hydrofoil HF-Sx at different Reynolds numbers.

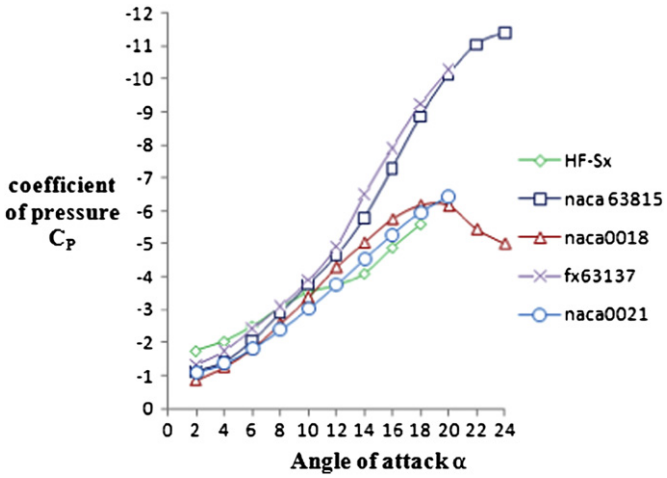

Fig. 12. Minimum coefficient of pressure for different hydrofoils at different angles of attack.

hydrofoils at different angles of attack can be seen from Figs. 13 and 14, it shows that the angle of attack for maximum C_L for other hydrofoils except HF-Sx is between 16° and 20°, therefore the L/D becomes very low at these angles of attack, as can be seen from Fig. 15. The hydrofoil NACA 63815 has been designed from NACA 63215 airfoil by increasing its camber four times; it has been used as a hydrofoil section for HAMCT and has been experimentally and numerically analyzed [7,12,13]. It has maximum lift at around AOA of 18°, around 1.56 and drag of around 0.071, as shown in Figs. 13

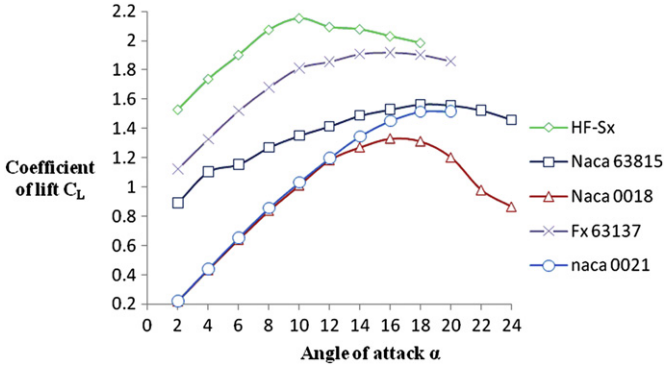

Fig. 13. Coefficient of lifts for different hydrofoils, at different angles at attack.

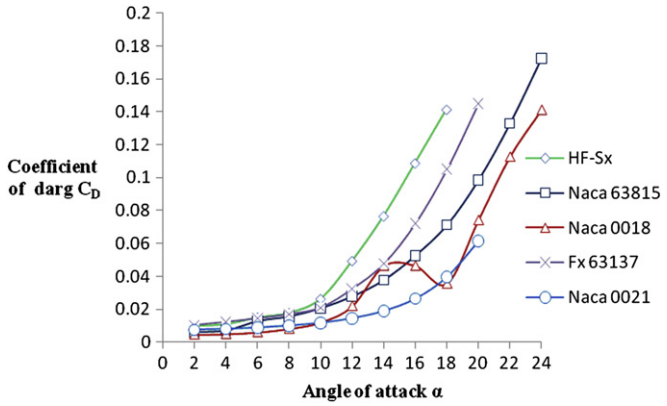

Fig. 14. Coefficient of drag for different hydrofoils, at different angles at attack.

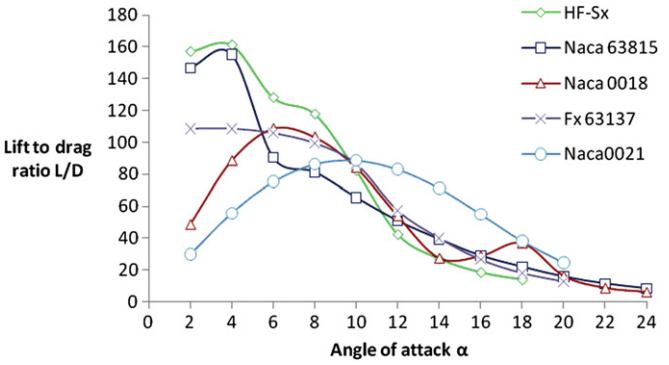

Fig. 15. Lift/Drag ratio for different hydrofoils, at different angles at attack.

and 14. Minimum C_P at maximum lift is around −8.9. There will be a chance of cavitation on the blade if maximum lift is being utilized for higher performance. NACA 0021 profile has been used as blade section for marine current turbines [14]. At maximum C_L, the minimum C_P is around −6.5, which is similar to NACA 63815; however, its L/D becomes very low (close to 20) which is not appropriate for designing a high-performance rotor. NACA 0018 has also been used for marine current blades; however, it has lower C_L lower C_P and L/D ratios [15]. FX63137 has been used as hydrofoil section for ducted marine current turbines [16]. It has higher C_L of 1.9 but it has very low L/D ratio of less than 20 and minimum C_P

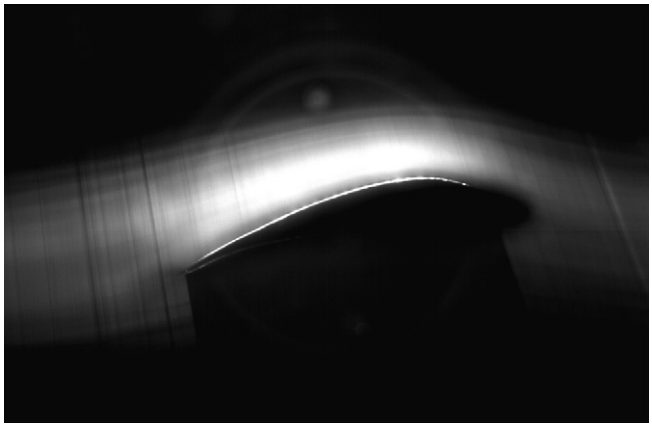

Fig. 16. Smoke test of HF-Sx at angle of attack of 6° and Reynolds number 190,000.

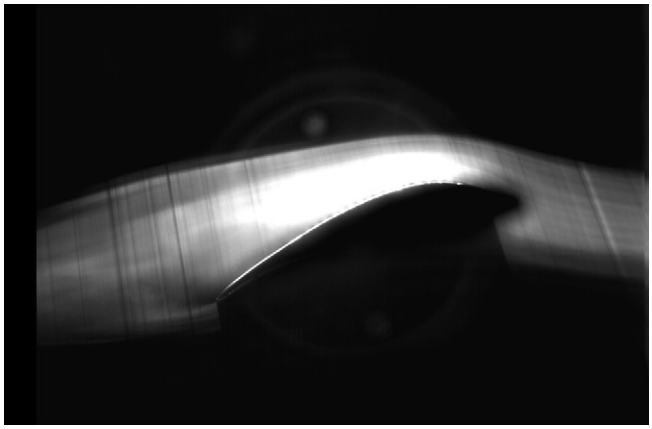

Fig. 17. Smoke test of HF-Sx at angle of attack of 12° and Reynolds number 190,000.

Table 2
Location of transition point, coefficient of skin friction drag and pressure drag at different angles of attack.

Reynolds number	Angle of attack	Location of transition point (% chord)	Coefficient of skin friction drag	Coefficient of pressure drag
1,835,381	5	0.3655	0.0568	0.00595
1,835,381	10	0.0902	0.00659	0.01981
2,240,651	5	0.3274	0.00572	0.00582
2,240,651	10	0.0762	0.0663	0.01942
2,341,035	5	0.3043	0.00592	0.00596
2,341,035	10	0.0738	0.00662	0.01923

of −9. However HF-Sx has significantly higher lift of around 2.2 at 11° AOA and higher L/D of around 80 and minimum C_P of −3.6, appropriate for high-performance rotor without having cavitation.

6. Location of free transition for HF-Sx

Transition or kink point is the point on the upper surface of the hydrofoil where the laminar boundary layer becomes turbulent. Turbulent boundary layer has more kinetic energy compared to laminar boundary layer therefore the flow separation gets delayed if the boundary layer becomes turbulent. The delayed flow separation has less pressure drag. Turbulent boundary layer results in lower pressure drag because of delayed separation; however it has a higher skin friction drag. Since pressure drag is greater compared to skin friction drag at the usual design angles, the overall drag reduces when separation is delayed. The transition point on the upper surface of hydrofoil HF-Sx was studied experimentally and by XFoil. Smoke test was done on the HF-Sx model in the wind tunnel to see the flow separation on the upper surface. Fig. 16 shows the smoke flow pattern on the HF-Sx hydrofoil at the Reynolds number of 190,000, and angle of attack of 6°. It can be seen that the flow is attached all the way to the trailing edge. Fig. 17 shows that there is no flow separation at the higher angle of attack of 12° as well. The transition point at 6° is at 47.64% of the chord; the coefficient of skin friction (c_{sf}) drag is 0.00592 and coefficient of pressure drag (c_{pd}) is 0.01897. As the angle of attack for a hydrofoil increases at a fixed Reynolds number, the skin friction drag increases because the location of transition moves toward the leading edge, increasing the turbulent boundary layer region; however, the pressure drag decreases especially at higher angles because the wake thickness reduces resulting in a reduction in momentum loss. The c_{pd} and c_{sf} at other Reynolds number can be seen in Table 2. As the Reynolds number increases for a fixed angle of attack, the c_{sf} increases and c_{pd} decreases because the transition point shifts more toward the leading edge.

7. Conclusion and recommendations

The hydrodynamic design of a hydrofoil is presented. The section characteristics are compared with other hydrofoils. HF-Sx can be used as an efficient hydrofoil for HAMCT. Cavitation is a major problem for HAMCT rotors; therefore it is appropriate to use lower TSR, while maximizing the number of blades to have higher hydrodynamic performance, increasing the camber and thickness of airfoils reduces the suction peak and also improves the performance. Designing the hydrofoil having lower suction peak and higher C_L and L/D will improve the rotor performance. A thicker blade section will provide good strength to the blade. For performance prediction there should be inclusion of modification to twist/pitch to account for non-uniform inflow (tidal profile and wave inception).

References

[1] Charlier RH. A “Sleeper” awakes: tidal current power. Renewable and Sustainable Energy Reviews 2003;7(3):187–213.
[2] Rourke FO, Boyle F, Reynolds A. Tidal energy update 2009. Ireland: Department of Mechanical Engineering; 2009.
[3] Bryden IG, Grinsted T, Melville GT. Assessing the potential of a simple tidal channel to deliver useful energy. Applied Ocean Research 2004;26(5): 198–204.
[4] Carlton JS. Marine propellers and propulsion. Butterworth Heinemann; 1994.
[5] Sale D, Jonlman J, Musial W. Hydrodynamic optimization method and design code for stall-regulated hydrokinetic turbine rotors. Hawaii: National Renewable Energy Laboratory; 2009.
[6] Guidance for Assessing Tidal Current Energy ANNEX II – Task 1.2 .2 generic and site relate ocean resources tidal data October 2008.
[7] Batten WMJ, Bahaj AS, Molland. AF, Chaplin. JR. Hydrodynamics of marine current turbine. Renewable Energy 2006;31:249–56.
[8] Drela M. XFoil: an analysis and design system for low Reynolds number airfoils. Conference on low Reynolds number airfoil aerodynamics. University of Notre Dame; 1989.
[9] Molland AF, Bahaj AS, Chaplin JR, Batten WMJ. Measurements and prediction of forces, pressure and cavitation on 2-D sections suitable for marine current turbines. Proceedings of the I MechE, Part M; 2004.
[10] Eisenberg P. Mechanics of cavitation. Hydronautics Incorporated; 1950.
[11] Barlow JB, Rae W, Pope H. A, low speed wind tunnel testing. 3rd ed. New York: John Wiley and Sons; 1999.
[12] Batten WMJ, Bahaj AS, Molland AF, Chaplin JR. The prediction of hydrodynamic performance of marine current turbines. Renewable Energy 2006;33: 1085–96.
[13] Bahaj AS, Molland AF, Chaplin JR, Batten WMJ. Power and thrust measurement of marine current turbines under hydrodynamic flow conditions in a cavitation tunnel and a towing tank. Renewable Energy 2007;32:407–26.
[14] Anders G, Staffan. L, Mats L. A parameter study of the influence of struts on the performance of a vertical-axis marine current turbine. Swedish Centre for Renewable Electric Energy Conversion. The Ångström Laboratory. Uppsala University; 2009.
[15] Zanette J, Imbault. D, Tourabi. A. Fluid Structure interaction and design of water current turbine. Scientific Bulletin of the "Politehnica" University of Timisoara Transactions on Mechanics 2007;(Fascicola 6). To52(66).
[16] Kirke B. Developments in ducted water current Turbines. Mawson Lakes, Australia: Sustainable Energy Centre, University of South Australia; 2006.